



## Discovery and in vivo evaluation of alcohol-containing benzothiazoles as potent dual-targeting bacterial DNA supercoiling inhibitors



James T. Palmer<sup>a,\*</sup>, Lorraine C. Axford<sup>a</sup>, Stephanie Barker<sup>b</sup>, James M. Bennett<sup>b</sup>, Michael Blair<sup>a</sup>, Ian Collins<sup>b</sup>, David T. Davies<sup>b</sup>, Leigh Ford<sup>a</sup>, Carlie T. Gannon<sup>a</sup>, Paul Lancett<sup>b</sup>, Alastair Logan<sup>b</sup>, Christopher J. Lunniss<sup>a</sup>, Craig J. Morton<sup>a</sup>, Daniel A. Offermann<sup>a</sup>, Gary R. W. Pitt<sup>a</sup>, B. Narasinga Rao<sup>c</sup>, Amit K. Singh<sup>c</sup>, Tarun Shukla<sup>c</sup>, Anil Srivastava<sup>c</sup>, Neil R. Stokes<sup>b</sup>, Helena B. Thomaidis-Brears<sup>b</sup>, Anju Yadav<sup>c</sup>, David J. Haydon<sup>b</sup>

<sup>a</sup> Biota Scientific Management, 10/585 Blackburn Road, Notting Hill, Victoria 3168, Australia

<sup>b</sup> Biota Europe Ltd, Begbroke Science Park, Begbroke, Oxfordshire OX51PF, United Kingdom

<sup>c</sup> Jubilant Chemsys Ltd, B-34, Sector 58, Noida 201301, India

### ARTICLE INFO

#### Article history:

Received 16 May 2014

Revised 10 July 2014

Accepted 14 July 2014

Available online 19 July 2014

#### Keywords:

DNA gyrase  
Topoisomerase  
Antibacterial  
Synthesis  
In vivo  
Dual-targeting

### ABSTRACT

A series of dual-targeting, alcohol-containing benzothiazoles has been identified with superior antibacterial activity and drug-like properties. Early lead benzothiazoles containing carboxylic acid moieties showed efficacy in a well-established in vivo model, but inferior drug-like properties demanded modifications of functionality capable of demonstrating superior efficacy. Eliminating the acid group in favor of hydrophilic alcohol moieties at C<sup>5</sup>, as well as incorporating solubilizing groups at the C<sup>7</sup> position of the core ring provided potent, broad-spectrum Gram-positive antibacterial activity, lower protein binding, and markedly improved efficacy in vivo.

© 2014 Elsevier Ltd. All rights reserved.

Increasing emergence of drug resistance in pathogenic bacteria has resulted in higher human mortality and increased healthcare costs.<sup>1,2</sup> We therefore targeted a new class of agents with no cross-resistance to existing therapies. Recently, we reported the discovery of a new class of dual-targeting, benzothiazole-containing small molecule inhibitors of bacterial DNA gyrase and topoisomerase IV.<sup>3</sup> Bacterial type II topoisomerases form heterotetramers consisting of two subunits: DNA gyrase forms an A<sub>2</sub>B<sub>2</sub> complex comprised of GyrA and GyrB, and topoisomerase IV forms a C<sub>2</sub>E<sub>2</sub> complex made up of ParC and ParE monomers.<sup>3</sup> In addition, the GyrB and ParE subunits are functionally similar with an ATPase active site within their N-terminal domains. The C-terminal domains of GyrB and ParE, by contrast, interact with the GyrA and ParC subunits of the heterotetramers, and also form the DNA binding grooves necessary for supercoiling and decatenation.<sup>4</sup> Highly conserved among bacterial species, these enzymes are ideal for broad spectrum inhibitor approaches. Fluoroquinolones inter-

act with the DNA binding grooves of the GyrA and ParC subunits, but the similarity between the ATP binding regions of GyrB and ParE suggests a motif for simultaneous targeting.<sup>5</sup> GyrB/ParE inhibitors offer the advantage of no pre-existing resistance and a low propensity for the development of resistance.

A number of groups have recently described ATP site-binding GyrB/ParE inhibitor series.<sup>6–10</sup> We recently reported the discovery of isonipecotic acid-containing benzothiazole ureas with enhanced solubility and pharmacokinetic properties,<sup>11,12</sup> along with microbiological assessment of well-characterized examples.<sup>13</sup> To establish the potential for further development of this chemotype, we evaluated compounds in a neutropenic mouse model of MSSA *Staphylococcus aureus* infection.<sup>14</sup> In this acute model, which was not designed to establish PK/PD parameters, compounds showed a dose-dependent drop in colony-forming units (CFUs) versus controls (Fig. 1).

Compounds **1** and **2** (MIC versus MSSA type strain *S. aureus* ATC 29213 of 0.06 and 0.12 µg/mL, respectively) were dosed intravenously at 2, 4, and 6 h after inoculation. Assessment of bacterial load 24 h post infection showed the compounds to have been efficacious. Although the lower doses of 3 × 30 mg/kg afforded

\* Corresponding author. Tel.: +61 3 9915 3700; fax: +61 3 9915 3701.

E-mail address: [j.palmer@biota.com.au](mailto:j.palmer@biota.com.au) (J.T. Palmer).

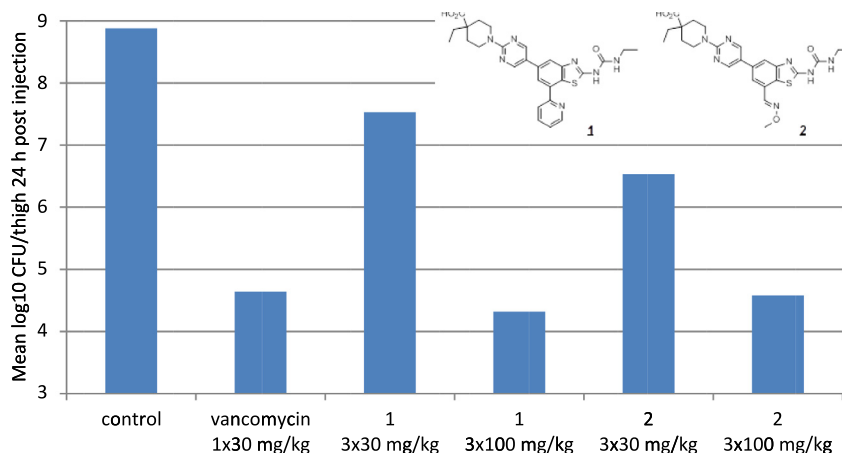


Figure 1. Efficacy of isonipecotic acids in neutropenic mouse thigh model.

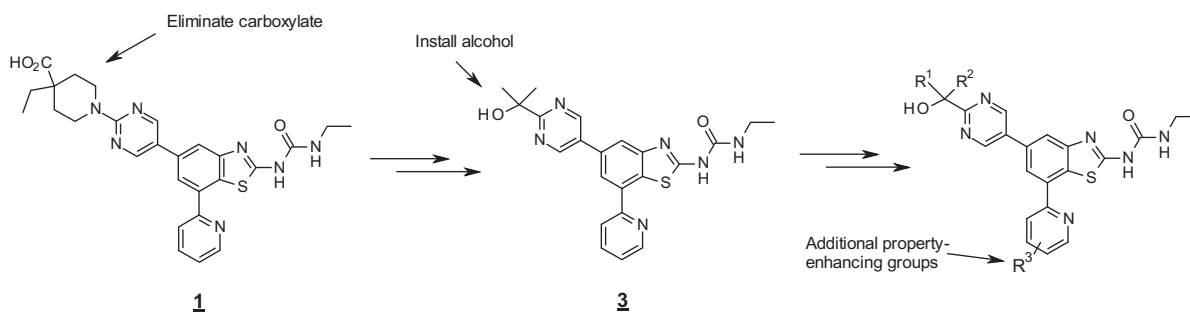
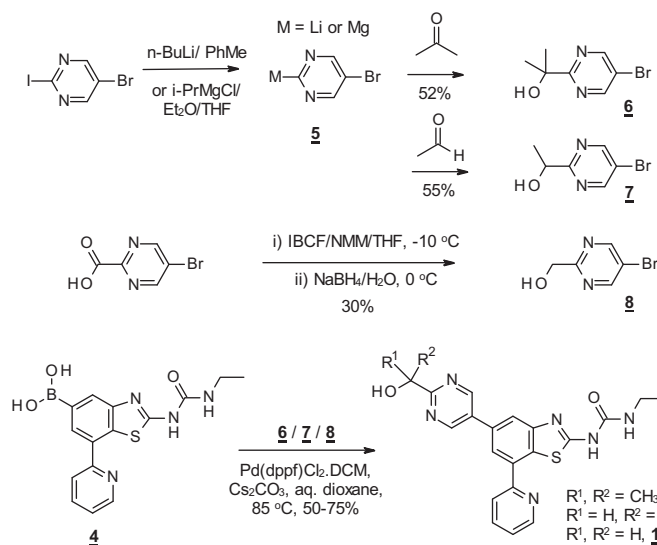


Figure 2. Evolution of alcohol-containing benzothiazole ureas.



Scheme 1. Synthesis of alcohol-containing C<sup>5</sup>-substituted benzothiazoles.

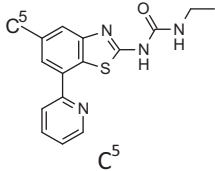
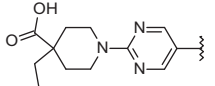
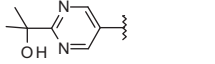
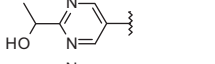
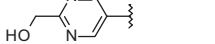
modest reductions in CFUs (<3 logs) the higher doses of  $3 \times 100$  mg/kg demonstrated greater than 4 log drops in CFUs, comparable to a single dose of vancomycin at 30 mg/kg. While calculating CFU reductions from an early time point is commonly used, it is not improper to calculate reductions from the matched control time point; when a compound has a static or slow cidal mode of action, calculating reductions in CFUs to the matched controls is more informative.<sup>6,14</sup>

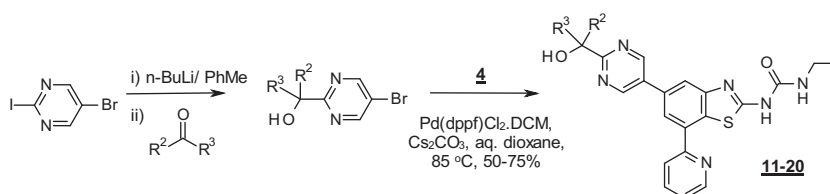
Armed with these encouraging proof-of-concept data, we sought to improve beneficial physical properties further. In particular, we

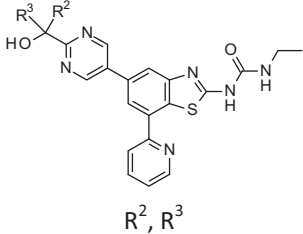
focused on reducing plasma protein binding, while retaining solubility sufficient to permit formulation within acceptable pH ranges for hospital-based intravenous administration. Lastly, we required demonstration of efficacy by both intravenous and oral routes, laying the groundwork for both inpatient and outpatient treatments.

To this end, we eliminated the carboxylic acid functionality in favor of an alcohol-substituted pyrimidine ( $R^1R^2COH$ ) attached to the C<sup>5</sup> position of the benzothiazole (Fig. 2). This moiety provided an alternative hydrophilic, yet neutral group suitable for prodrugging as needed. At the same time, we recognized a further

**Table 1**  
Antibacterial (MIC) activity of alcohol-containing benzothiazole compounds

Entry		<i>S. aureus</i> 29213 <sup>a</sup>	<i>S. pyogenes</i> 51339 <sup>a</sup>	<i>H. influenzae</i> 49247 <sup>a</sup>	<i>S. aureus</i> T173 N (GyrB) <sup>a,b</sup>	<i>S. pyogenes</i> A53S (ParE) <sup>a,b</sup>	<i>S. aureus</i> 29213 + 50% horse serum <sup>a</sup> (shift)
<b>1</b>		0.06	0.06	4	0.25	0.5	4 (64×)
<b>3</b>		0.06	0.12	1	0.25	1	0.25 (4×)
<b>9</b>		0.03	0.06	0.5	0.25	1	0.12 (4×)
<b>10</b>		0.03	0.06	0.25	0.25	0.5	0.06 (2×)

<sup>a</sup> µg/mL.<sup>b</sup> See Refs. 11,13 for methodology.**Scheme 2.** Preparation of tertiary alcohol-containing benzothiazole ureas.**Table 2**  
Biochemical, antibacterial activity of tertiary alcohol-based benzothiazole ureas

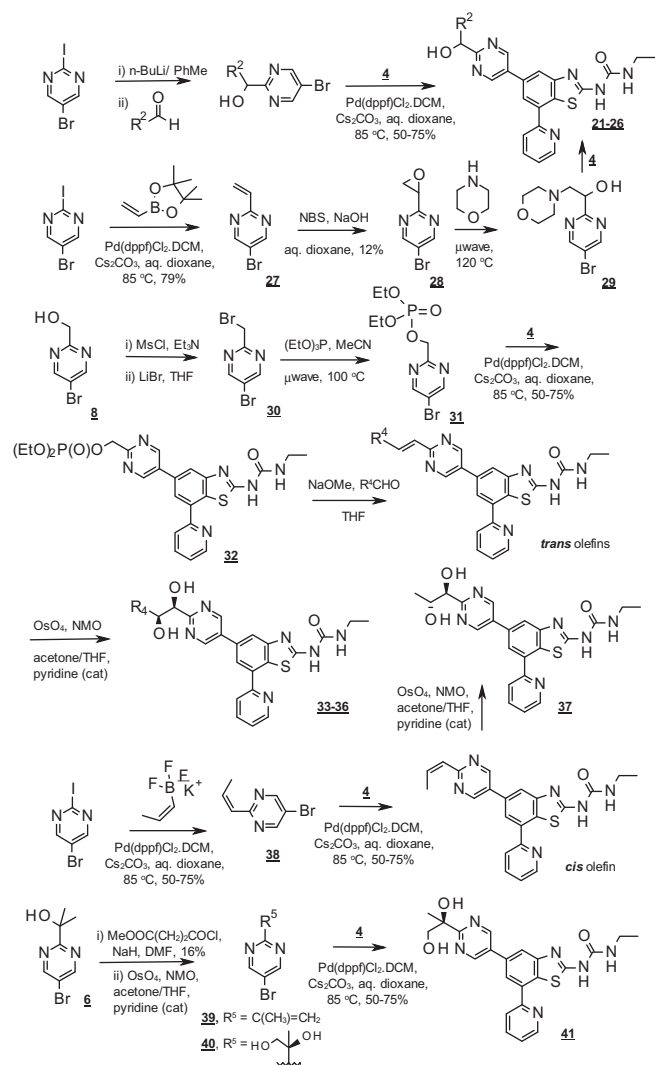
Entry		<i>S. aureus</i> GyrB ATPase <sup>a</sup>	<i>S. aureus</i> 29213 <sup>a</sup>	<i>S. pyogenes</i> 51339 <sup>a</sup>	<i>H. influenzae</i> 49247 <sup>a</sup>	<i>S. aureus</i> T173 N (GyrB) <sup>a</sup>	<i>S. pyogenes</i> A53S (ParE) <sup>a</sup>	<i>S. aureus</i> 29213 + 50% horse serum <sup>a</sup>
<b>3</b>	(CH <sub>3</sub> ) <sub>2</sub>	0.006	0.06	0.12	1	0.25	1	0.25
<b>11</b>	(CH <sub>3</sub> CH <sub>2</sub> ) <sub>2</sub>	0.017	0.25	0.5	8	1	8	4
<b>12</b>	-(CH <sub>2</sub> ) <sub>4</sub> -	0.005	0.03	0.12	1	0.25	2	0.5
<b>13</b>	-(CH <sub>2</sub> ) <sub>5</sub> -	0.054	8	8	> 16	> 16	> 16	16
<b>14</b>	-(CH <sub>2</sub> CH <sub>2</sub> OCH <sub>2</sub> CH <sub>2</sub> )-	0.005	0.06	0.12	1	0.25	2	0.12
<b>15</b>	-(CH <sub>2</sub> CH <sub>2</sub> SO <sub>2</sub> CH <sub>2</sub> CH <sub>2</sub> )-	0.005	0.12	0.5	2	0.25	4	1
<b>16</b>	-(CH <sub>2</sub> CH <sub>2</sub> SO <sub>2</sub> CH <sub>2</sub> CH <sub>2</sub> )-	0.006	0.25	0.25	1	1	2	0.5
<b>17</b>	-(CH <sub>2</sub> CH <sub>2</sub> N(CH <sub>3</sub> )CH <sub>2</sub> CH <sub>2</sub> )-	0.011	1	1	8	8	8	0.5
<b>18</b>	-(CH <sub>2</sub> CH <sub>2</sub> NHCH <sub>2</sub> CH <sub>2</sub> )-	0.010	8	2	> 16	> 16	> 16	4
<b>19</b>	-(CH <sub>2</sub> NHCH <sub>2</sub> )-	0.029	> 16	8	> 16	> 16	> 16	> 16
<b>20</b>	-(CH <sub>2</sub> OCH <sub>2</sub> )-	0.006	0.06	0.12	0.5	0.5	2	0.12

<sup>a</sup> µg/mL.

opportunity to reduce protein binding by substituting on the C<sup>7</sup> heterocycle (R<sup>3</sup>).

Preparation of **3**, and secondary and primary alcohol analogs **9** and **10** respectively, utilized our established core synthesis method to couple boronic acid **4**<sup>3</sup> with an appropriately functionalized

heterocycle. Thus, as depicted in [Scheme 1](#), metalation of 2-iodo-5-bromopyridine gave **5**, followed by acetone quenching, delivered the tertiary alcohol **6**. Palladium-catalyzed cross-coupling of **6** with **4** yielded **3** in good yields. Likewise, quenching of the anionic **5** with acetaldehyde delivered secondary alcohol **7**. Sodium



**Scheme 3.** Preparation of secondary alcohol, diol-containing benzothiazole ureas. borohydride-mediated reduction of the mixed anhydride of 5-bromopyrimidine-2-carboxylic acid and isobutyl chloroformate, in the presence of *N*-methylmorpholine, afforded primary alcohol **8**.

SAR for this series illustrated that alcohol-containing compounds had potent antibacterial activity against a primary panel

of target pathogens, compared directly with carboxylic acid **1** (Table 1).

Notably, the antibacterial activity remained consistent irrespective of the distal C<sup>5</sup> substituent, whether acidic or alcoholic. Modeling of the series within the active site of the *Escherichia coli* enzymes suggested neither moiety would interfere with binding in the ATPase pockets of either GyrB or ParE.<sup>15</sup> The characterization of first-step mutants (*S. aureus* GyrB T173 N and *Streptococcus pyogenes* ParE A53S) indicated that the primary target is GyrB in *S. aureus* and ParE in *S. pyogenes*.<sup>13</sup> The retention of sub-μg/mL MIC values against these strains indicate that the compounds also inhibit the secondary targets, ParE and GyrB respectively, reflecting potential for dual targeting. Activity (4 μg/mL) against a double mutant of *S. aureus* 29213 (GyrB T173N, ParE T167N) for **3** and **9** further illustrate the dual targeting potential of representative compounds. In addition, the serum shift observed when compounds were assessed for anti-staphylococcal activity in the presence of 50% horse serum was greatly diminished, illustrating the improvement in protein binding properties.

To explore the scope and limitations of the alcohol-containing substituent, we prepared an additional series of C<sup>5</sup> alcohols. Lithiation of 2-iodo-5-bromopyrimidine, followed by quenching by the relevant ketone, afforded tertiary alcohol-containing C<sup>5</sup> moieties suitable for Pd-mediated cross-coupling with boronic acid **4** (Scheme 2).

We observed subtle steric constraints upon assaying this series against the primary pathogen panel (Table 2). Consistently, the series proved to show good on-target potency against DNA gyrase ATPase, as measured in a malachite green assay format,<sup>16</sup> with all examples tested displaying double digit ng/mL potency or better.

Introduction of bulk at the tertiary, pseudobenzyl position off the pyrimidine ring (diethyl, **11**, and cyclohexyl ring system, **13**) resulted in a loss of activity, particularly against the ParE mutant strain of *S. pyogenes*. For **13**, both biochemical and antibacterial activities were significantly reduced compared to other members of the series. Introduction of a heteroatom into the alicyclic 6-membered ring (**14–18**), however, increased on-target ATPase inhibition, suggesting a subtle conformational role, possibly a flattening of the ring. Bacterial membrane penetration was reduced in the piperazine containing examples (**17**, **18**), the effect more pronounced for the secondary amine. Contraction of the ring to an azetidine (**19**), leaving the free NH group more exposed, reduced antibacterial activity further. However, the physically constrained oxetane analog **20** displayed strong potency across the entire

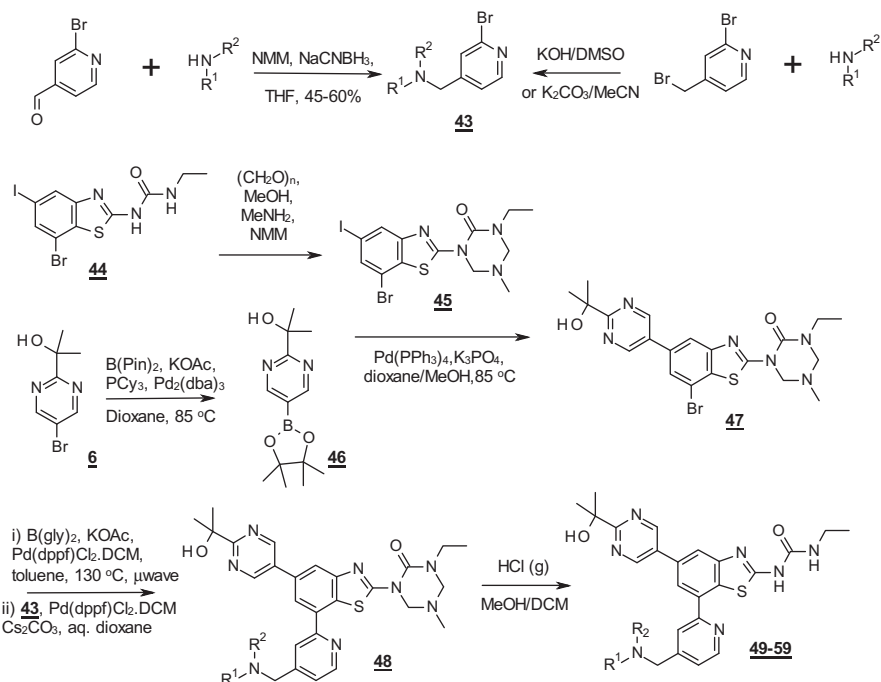
**Table 3A**  
Biochemical, antibacterial activity of secondary alcohol-based benzothiazole ureas

Entry		<i>S. aureus</i> GyrB ATPase <sup>a</sup>	<i>S. aureus</i> 29213 <sup>a</sup>	<i>S. pyogenes</i> 51339 <sup>a</sup>	<i>H. influenzae</i> 49247 <sup>a</sup>	<i>S. aureus</i> T173 N (GyrB) <sup>a</sup>	<i>S. pyogenes</i> A53S (ParE) <sup>a</sup>	<i>S. aureus</i> 29213 + 50% horse serum <sup>a</sup>
<b>21</b>	Et–	0.006	0.06	0.06	1	0.25	1	0.25
<b>22</b>	<i>n</i> -Pr–	0.007	0.03	0.06	1	0.25	2	0.25
<b>23</b>	<i>tert</i> -Bu–	0.012	0.12	0.12	16	0.25	2	2
<b>24</b>	cyclo-Pr–	0.008	0.06	0.06	0.5	0.25	1	0.25
<b>25</b>	HOCH <sub>2</sub> –	0.006	0.12	0.12	0.5	2	2	0.5
<b>26</b>	O(CH <sub>2</sub> CH <sub>2</sub> ) <sub>2</sub> NCH <sub>2</sub> –	0.011	0.12	0.12	2	1	2	0.25

<sup>a</sup> μg/mL.

**Table 3B**  
Biochemical, antibacterial activity of diol-containing benzothiazole ureas

Entry		<i>S. aureus</i> GyrB ATPase <sup>a</sup>	<i>S. aureus</i> 29213 <sup>a</sup>	<i>S. pyogenes</i> 51339 <sup>a</sup>	<i>H. influenzae</i> 49247 <sup>a</sup>	<i>S. aureus</i> T173 N (GyrB) <sup>a</sup>	<i>S. pyogenes</i> A53S (ParE) <sup>a</sup>	<i>S. aureus</i> 29213 + 50% horse serum <sup>a</sup>
	R <sup>4</sup>							
<b>33</b>		0.007	0.25	0.12	1	1	1	0.25
<b>34</b>		0.004	0.06	0.12	0.25	0.5	1	0.25
<b>35</b>		0.005	0.06	0.12	0.5	0.25	1	0.25
<b>36</b>		0.009	0.5	0.12	2	4	2	0.5
<b>37</b>		0.004	0.12	0.12	0.5	0.5	1	0.25
<b>42</b>		0.006	0.12	0.12	0.5	1	2	0.25

<sup>a</sup> μg/mL.**Scheme 4.** Preparation of C<sup>7</sup>-modified benzothiazole ureas.

panel, with only a modest two-fold shift in MIC in the presence of 50% horse serum.

Discovery of this possible steric constraint around the pyrimidine C<sup>5</sup> appendage prompted us to explore additional secondary alcohol and diol-containing molecules with further solubility enhancement potential. While this approach introduced latent

complications of additional chiral centers, we chose initially to work within the racemic series (Scheme 3). For simple secondary alcohols, the building blocks were available through aldehyde quenching of 5-bromo-2-lithiopyrimidine as illustrated above. Suzuki coupling with **4** once again delivered final products **21–25** in good yields. The morpholine derivative **26** came from Suzuki

**Table 4**  
Further profiling of C<sup>7</sup>-modified benzothiazole ureas

Entry		<i>S. aureus</i> GyrB ATPase <sup>a</sup>	<i>S. aureus</i> 29213 <sup>a</sup>	<i>S. pyogenes</i> 51339 <sup>a</sup>	<i>H. influenzae</i> 49247 <sup>a</sup>	<i>S. aureus</i> 29213 + 50% horse serum <sup>a</sup>	Mouse PPB (FU) <sup>b</sup> (%)
<b>3</b>		0.006	0.06	0.12	1	0.25	5.1
<b>49</b>		0.012	0.5	0.5	4	0.5	6.7
<b>50</b>		0.005	0.06	0.06	1	0.25	6.3
<b>51</b>		0.008	0.12	0.06	2	0.25	6.1
<b>52</b>		0.007	0.06	0.03	> 16	0.25	4.1
<b>53</b>		0.006	0.12	0.12	2	0.25	5.6
<b>54</b>		0.009	0.25	0.25	4	0.5	9.0
<b>55</b>		0.007	0.5	0.25	4	0.5	19.4
<b>56</b>		0.008	0.5	0.25	8	0.25	19.4
<b>57</b>		0.011	0.12	0.12	2	0.25	11.0
<b>58</b>		0.004	1	0.25	2	1	22.0
<b>59</b>		0.011	0.5	0.12	4	0.5	22.3

<sup>a</sup> µg/mL.

<sup>b</sup> See footnote 19 for methodology.

vinylation of the pyrimidine (**27**), epoxide formation (**28**), opening to building block **29**, and finally coupling with the core. For diols derived from *trans*-olefins, the building blocks came from primary alcohol **8**, which we converted to the bromomethylpyridine bromide **30** via the isolated mesylate. Arbuzov replacement with triethyl phosphite gave Wadsworth–Horner–Emmons precursor **31**, which underwent Suzuki coupling with **4** to give **32**. Olefination with aldehydes afforded *trans*-olefins, which underwent *cis*-dihydroxylation<sup>17</sup> in the presence of OsO<sub>4</sub> to give the final products **33–36**. We prepared *trans*-diol **37** first by assembling the *cis*-olefin-based building block via Suzuki reaction between 2-iodo-5-bromopyridine and the trifluoroborate of 2-propene, coupling **38** with **4**, and dihydroxylation of the *cis*-olefin. Finally, we made tertiary diol **41** from **8** in a multi-step procedure, first by conversion to its methoxysuccinyl ester, which underwent E2 elimination under reaction conditions to form **39** as a by-product. Dihydroxylation and coupling with **4** as before completed the synthesis.

Tables 3A and 3B illustrate the profile of compounds within this subset of compounds. Extension of R<sup>2</sup> to longer chain alkyl and small cycloalkyl groups (**21**, **22**, **24**) had virtually no effect on the potency of the series towards the enzyme. Echoing our earlier observations for bulkier rings in the tertiary series, the large *t*-butyl moiety (**23**) gave a substantial drop in activity against *Haemophilus influenzae*, for reasons not readily apparent, although we also observed a concomitant drop in activity against *S. aureus* in the presence of serum. The loss of permeability of the lipooligosaccharide-containing outer membrane of this Gram-negative bacterium is one possible explanation. The morpholine group **26**, designed to enhance hydrophilicity, was reasonably well tolerated, as was diol **25**.

Extension of the diol-containing series is illustrated in Table 3B. Once again, the introduction of small groups did not hamper on-target or antimicrobial activity significantly, but diol **36** once again illustrated the relative intolerance of larger rings. Particularly

encouraging, however, was the high level of potency seen in the presence of serum, suggesting that protein binding within the series was reduced or rapidly reversible. Lastly, while the examples in Table 3B all reflected racemic compounds, there appeared to be little, if any effect on diol geometry; the *cis*-diol **35** (resulting from the *trans*-olefin) was within a doubling dilution of its *trans*-diol analog **37**. Further exploration of the chiral versions of the alcohol series will be the subject of a future report.

We next turned our attention to the C<sup>7</sup> portion of the benzothiazole core. Since the alcohol moiety was well-tolerated, we chose the *gem*-dimethylcarbinol moiety of **3** as the starting point for our exploration. By incorporating further property enhancing groups (e.g., mildly basic moieties capable of forming salts, Fig. 2) designed not to interfere with binding, we targeted improved solubility and lower intrinsic plasma protein binding. Preparation of the C<sup>7</sup>-modifications followed a convergent approach (Scheme 4) wherein the C<sup>7</sup> moieties arose either from reductive aminations of 2-bromo-4-formylpyridine or amine displacement of 2-bromo-4-bromomethylpyridine to yield building blocks **43**. We prepared the triazone **45**<sup>18</sup> in near quantitative yields by incubating **44** with paraformaldehyde and methanolic methylamine under basic conditions, which then smoothly coupled with boronate **46**, available directly from precursor **6**. C<sup>7</sup> bromide **47** underwent a two-step conversion, first to the unisolated glycolatoboron ester under microwave conditions, and then subsequent Suzuki coupling with building blocks **43** to yield the fully elaborated triazones, represented as **48**. Release of the final products **49–59** came via HCl deprotection of the triazones in DCM/methanol.

We further assessed examples in this series in an ultracentrifugation-based protein binding assay<sup>19</sup> in the presence of mouse plasma, chosen to inform the potential for subsequent animal efficacy studies. The introduction of basic groups significantly increased the unbound fraction (FU), while maintaining high on-target potency and low MICs against Gram-positive targets (Table 4).

Notably, while we observed consistently good activity against the GyrB ATPase of *S. aureus* and low MIC values against both *S. aureus* and *S. pyogenes*, we saw a drop-off of activity against *H. influenzae* (values ranging from 1 to >16 µg/mL) thus suggesting either a change in permeability properties or efflux. We also observed a limited reduction in activity against the *S. pyogenes* A53S (ParE) mutant strain, but still observed single-digit µg/mL potency within the series. Activity against the *S. aureus* T173N (GyrB) mutant strain remained at single digit µg/mL or less, the hallmark of dual-targeting, indicating a low overall propensity for developing resistance. Gratifyingly, we achieved an increase in free fraction within the series; the installation of 5-membered rings further substituted with ether or alcohol containing moieties (**54–56**) increased the unbound fraction from 9 to 19%, although this enhancement was partially offset by a moderate increase in MIC. Azetidine-containing examples **57–59** enhanced this property even further, giving us optimism for further in vivo testing with a regimen wherein lower or less frequent dosing would be required.

To assess the efficacy of our compounds, we initially chose **3** as a proof-of-concept example, with a moderate free fraction (5.1% unbound) and a strong antibacterial profile, in the aforementioned neutropenic mouse thigh model. Again, mice inoculated with  $\sim 2 \times 10^5$  CFUs of *S. aureus* (ATCC 19636) were given a single dose of test compound at 30 mg/kg (intravenously) and 100 mg/kg (oral gavage), using identical formulation conditions for both routes. We included two control compounds, novobiocin, with a similar mechanism of action to our series, and linezolid, as the current standard of care in Gram-positive infections. Figure 3 indicates the results in this Letter.

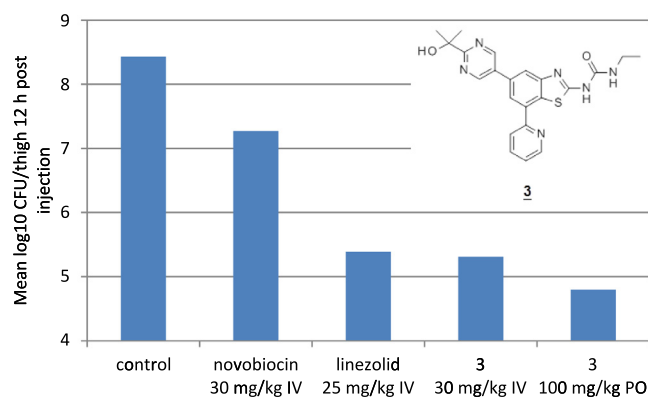


Figure 3. Improved efficacy in the neutropenic mouse thigh model.

We were pleased to observe that not only was **3** effective in this model by both oral and intravenous routes, but it showed comparable efficacy to linezolid and superior efficacy than novobiocin. Moreover, the study was conducted with a single dose of **3**, as compared to our earlier experiment requiring multiple dosing of carboxylic acids **1** and **2**. Pharmacokinetic parameters for **3** in the mouse<sup>20</sup> revealed a bioavailability of 34%, consistent with the observed drops in CFU values for the two routes of administration.

In conclusion, introduction of alcohol-containing moieties at the C<sup>5</sup> position of the benzothiazole series, along with modifications at the C<sup>7</sup> position designed to enhance hydrophilicity and reduce protein binding, yielded significant enhancements to an established core with potent Gram-positive antibacterial activity. The observation of proof-of-concept efficacy, at least as good as the marketed standard of care, in a gold-standard, high hurdle, model of infection via both intravenous and oral dosing, suggests that this series is suitable for further enhancement towards clinical development for both hospitalized and outpatient groups. Further details on this series will be published in due course.

## References and notes

- Magiorakos, A.-P.; Srinivasan, A.; Carey, R. B.; Carmeli, Y.; Falagas, M. E.; Giske, C. G.; Harbarth, S.; Hindler, J. F.; Kahlmeter, G.; Olsson-Liljequist, B.; Paterson, D. L.; Rice, L. B.; Stelling, J.; Struelens, M. J.; Vatopoulos, A.; Weber, J. T.; Monnet, D. L. *Clin. Microbiol. Infect.* **2012**, *18*, 268.
- Silver, L. L. *Clin. Microbiol. Rev.* **2011**, *24*, 71.
- Haydon, D. J.; Czaplewski, L. G.; Palmer, N. G.; Mitchell, F. R.; Atherall, J. F.; Steele, C. R.; Ladduwahetty, T., U.S. Patent # 7,977,340.
- a) Maxwell, A. *Nat. Struct. Biol.* **1996**, *3*, 109; b) Wang, J. *Quart. Rev. Biophys.* **1998**, *31*, 107; c) Drlaca, K.; Zhao, X. *Microbiol. Mol. Biol. Rev.* **1997**, *61*, 377; (d) Laponogov, I.; Veselkov, D. A.; Sohi, M. K.; Pan, X.-S.; Achari, A.; Yang, C.; Ferrara, J. D.; Fisher, L. M.; Sanderson, M. R. *PLoS One* **2007**, *2*, e301. <http://dx.doi.org/10.1371/journal.pone.0000301>.
- Collin, F.; Karkare, S.; Maxwell, A. *Appl. Microbiol. Biotechnol.* **2011**, *92*, 479.
- Charifon, P. S.; Grillot, A.-L.; Grossman, T. H.; Parsons, J. D.; Badia, M.; Bellon, S.; Deininger, D. D.; Drumm, J. E.; Gross, C. H.; LeTiran, A.; Liao, Y.; Mani, N.; Nicolau, D. O.; Perola, E.; Ronkin, A.; Shannon, D.; Swenson, L. L.; Tang, Q.; Tessier, P. R.; Tian, S.-K.; Trudeau, M.; Wang, T.; Wei, Y.; Zhang, H.; Stamos, D. J. *Med. Chem.* **2008**, *51*, 5243.
- East, S. P.; White, C. B.; Barker, O.; Barker, S.; Bennett, J. M.; Brown, D.; Boyd, E. A.; Brennan, C.; Chowdhury, C.; Collins, I.; Convers-Reignier, E.; Dymock, B. W.; Fletcher, R.; Haydon, D. J.; Gardiner, M.; Hatcher, S.; Ingram, P.; Lancett, P.; Mortenson, P.; Papadopoulos, K.; Smece, C.; Thomaidis-Brears, H. B.; Tye, H.; Workman, J.; Czaplewski, L. G. *Bioorg. Med. Chem. Lett.* **2009**, *19*, 894.
- Starr, J. T.; Sciotti, R. J.; Hanna, D. L.; Huband, M. D.; Mullins, L. M.; Cai, H.; Gage, J. W.; Lockard, M.; Rauckhorst, M. R.; Owen, R. M.; Lall, M. S.; Tomilo, M.; Chen, H.; McCurdy, S. P.; Barbachyn, M. R. *Bioorg. Med. Chem. Lett.* **2009**, *19*, 5302.
- Tari, L. W.; Trzoss, M.; Bensen, D. C.; Li, X.; Chen, Z.; Lam, T.; Creighton, C. J.; Cunningham, M. L.; Kwan, B.; Stidham, M.; Shaw, K. J.; Lightstone, F. C.; Wong, S. E.; Nguyen, T. B.; Nix, J.; Finn, J. *Bioorg. Med. Chem. Lett.* **2013**, *23*, 1529.
- Tari, L. W.; Li, X.; Trzoss, M.; Bensen, D. C.; Chen, Z.; Lam, T.; Zhang, J.; Lee, S. J.; Hough, G.; Phillipson, D.; Akers-Rodriguez, S.; Cunningham, M. L.; Kwan, B. P.; Nelson, K. J.; Castellano, A.; Locke, J. B.; Brown-Driver, V.; Murphy, T. M.; Ong, V. S.; Pillar, C. M.; Shinabarger, D. L.; Nix, J.; Lightstone, F. C.; Wong, S. E.

- Nguyen, T. B.; Shaw, K. J.; Finn, J. *PLoS One* **2013**, 8(12), e84409. <http://dx.doi.org/10.1371/journal.pone.0084409>.
11. Axford, L. C.; Agarwal, P. K.; Anderson, K. H.; Andrau, L. N.; Atherall, J.; Barker, S.; Bennett, J. M.; Blair, M.; Collins, I.; Czaplowski, L. G.; Davies, D. T.; Gannon, C. T.; Kumar, D.; Lancett, P.; Logan, A.; Lunniss, C. J.; Mitchell, D. R.; Offermann, D. A.; Palmer, J. T.; Palmer, N.; Pitt, G. R. W.; Pommier, S.; Price, D.; Rao, B. N.; Saxena, R.; Shukla, T.; Singh, A. K.; Singh, M.; Srivastava, A.; Steele, C.; Stokes, N. R.; Thomaidis-Brears, H. B.; Tyndall, E. M.; Watson, D.; Haydon, D. J. *Bioorg. Med. Chem. Lett.* **2013**, 23, 6598.
  12. Palmer, J.T.; Lunniss, C.L.; Offermann, D.A.; Axford, L.C.; Blair, M.; Mitchell, D.; Palmer, N.; Steele, C.; Atherall, J.; Watson, D.; Haydon, D.; Czaplowski, L.; Davies, D.; Collins, I.; Tyndall, E.M.; Andrau, L.; Pitt, G.R.W.; PCT Int. Appl. WO2012/045124.
  13. Stokes, N. R.; Thomaidis-Brears, H. B.; Barker, S.; Bennett, J. M.; Berry, J.; Collins, I.; Czaplowski, L. G.; Gamble, V.; Lancett, P.; Logan, A.; Lunniss, C. J.; Peasley, H.; Pommier, S.; Price, D.; Smee, C.; Haydon, D. J. *Antimicrob. Agents Chemother.* **2013**, 57, 5977.
  14. Weiss, W. J.; Murphy, T.; Lenoy, E.; Young, M. *Antimicrob. Agents Chemother.* **2004**, 48, 1708. Thighs of female CD-1 mice (18–22 g) rendered neutropenic by the intraperitoneal administration of cyclophosphamide (150 mg/kg at day-4 and 100 mg/kg at day -1) were inoculated with approximately  $2 \times 10^5$  CFUs of MSSA type strain *S. aureus* (ATCC 19636) prepared from a fresh overnight culture. Compounds were administered at two hour intervals (2, 4, 6 h post inoculation) and CFUs enumerated at 24 h post dosing by harvesting the thighs, homogenizing in saline on ice, and plating serial dilutions onto charcoal containing plates for growth overnight and colony counting. MIC values for *S. aureus* type strains ATCC 29213 and ATCC 19636 have been consistent within this compound series.
  15. (a) Unpublished results; (b) PDB ID: 3FV5; Wei, L.; Letiran, A. Design and synthesis of novel C7-derived aminobenzimidazole ureas: bacterial gyrase/topoisomerase IV inhibitors with potent Gram-positive antibacterial activity.
  16. ATPase assay: enzymes were purchased from Inspiralis Ltd. (Norwich, United Kingdom). For the *S. aureus* DNA gyrase ATPase assay, the final assay composition was 10 nM DNA gyrase enzyme ( $A_2B_2$  complex), 0.08 mg/mL DNA, 40 mM HEPES pH 7.6, 10 mM magnesium acetate, 0.5 M potassium glutamate, 0.01 mg/mL BSA and 2 mM DTT, 1 mM ATP and 5% DMSO solution containing the compounds. For the *S. aureus* topoisomerase IV ATPase assay, the final assay composition was 25 nM topoisomerase IV enzyme ( $C_2E_2$  complex), 0.01 mg/mL DNA, 50 mM Tris-HCl pH 7.5, 5 mM magnesium chloride, 0.35 M potassium glutamate, 0.05 mg/mL BSA and 5 mM DTT, 1 mM ATP and 1% DMSO solution containing the compounds. The reactions, in a volume of 25  $\mu$ L, were started by the addition of the ATP and allowed to incubate at 30 °C for 60 min. Reactions were stopped by adding 0.2 mL malachite green solution (0.034% malachite green, 10 mM ammonium molybdate, 1 M HCl, 3.4% ethanol, 0.01% tween 20). Color was allowed to develop for 5 min and the absorbance at 600 nm was measured spectrophotometrically. The half-maximum inhibitory concentration ( $IC_{50}$ ) values were determined from the absorbance readings using no compound and no enzyme controls. The assay sensitivity limits of this assay preclude precise values <0.005  $\mu$ g/mL.
  17. VanRheenen, V.; Kelly, R. C.; Cha, D. Y. *Tetrahedron Lett.* **1973**, 1976, 17.
  18. Knapp, S.; Hale, J. J.; Bastos, M.; Gibson, F. *Tetrahedron Lett.* **1990**, 31, 2109.
  19. Protein binding was measured using a centrifugation method and neat plasma. Compounds were tested at 10  $\mu$ M (1% DMSO), and allowed to equilibrate at 37 °C for 60 min. Two aliquots of each sample were subjected to ultracentrifugation (250,000g for 4.2 h at 37 °C to separate plasma proteins from plasma water. 50  $\mu$ L supernatant (plasma water) was sampled per tube to determine the free compound concentration, compared to samples that had not been centrifuged but were subject to the same incubation period. Compound degradation was assessed by testing samples that had not been centrifuged and kept at –20 °C. Diltiazem was used as a stability control and has plasma instability over the incubation period. Supernatants were analyzed using LCMS.
  20. Swiss male albino mice were assessed via intravenous dose formulation (10% DMSO, 40% TEG, 10% HP $\beta$ CD), administered as a single bolus dose through tail vein at dose level of 3 mg/kg, and via oral dose formulation (10% DMSO, 40% TEG, 10% HP $\beta$ CD) by oral gavage needle at dose level of 3 mg/kg. Dose volumes were 5 mL/kg. Sampling time points were pre-dose, 0.08, 0.25, 0.5, 1, 2, 4, and 8 h. Calculated pharmacokinetic parameters were as follows: IV dosing:  $C_0$  = 7.4  $\mu$ g/mL; AUC (0–8 h) = 11.9  $\mu$ g h/mL;  $t_{1/2}$  = 68 min; CL = 0.5 mL/min/kg;  $V_d$  = 0.4 L/kg. PO dosing:  $C_{max}$  = 2.1  $\mu$ g/mL; AUC (0–8 h) = 2.1  $\mu$ g h/mL;  $t_{1/2}$  = 97 min; F = 34%.